CMEBM Project: *A multidimensional model for the Ca^{2+} ion dynamics in the astrocytes*

Thomas Bellotti - Politecnico di Milano
Project advisor: *Prof. Aurelio Giancarlo Mauri*

October 1, 2019

Abstract

Astrocytes are an important kind of cell in the central nervous system, often acting as a regulatory device. For example, the glutamate stimulus indirectly modifies the calcium concentration by increasing the availability of inositol trisphosphate which stimulates the endoplasmatic reticulum to release calcium ions into the cytoplasm. The incrase of calcium triggers the release of arachidonic acid from the membrane, with many consequences on the blood flow in the surrouding tissues.

We provide a highly simplified space-extended model to study the dynamics of Ca^{2+} ions released thanks to inositol trisphosphate. It accounts for the calcium flux through transmembrane calcium channels induced by the difference of concentration and for the calcium release from the channels localized over the endoplasmatic reticulum membrane, modulated by the level of inositol trisphosphate produced by the glutamate receptors. This phenomena are modeled in terms of time varying local boundary conditions and the concentrations of both species satisfy a diffusion equation. We propose a discretization of our model by Finite Differences in time and Finite Elements in space.

Contents

1 Introduction

1.1 The subject and a brief state of the art

Studying the dynamics of the Ca^{2+} ions in cells, especially in astrocytes, is a crucial research topic in biology. Indeed, astrocytes are the predominant kind of glia cell in the central nervous system, though there is no unanimous definition of them, due to their heterogeneity. These cells have many important functions and two of them especially drew our attention:

- They "remove" the excess of glutamate, which is one of the most important neurotransmitter for vertebrates but can become a neurotoxin when present in excessive quantity for a long lapse of time.

- They trigger the release of Ca^{2+} ions, which can constitute a signal for controlling the neurovascular unit. In particular, these signals induce significant modifications in the radii of the arterioles (see [8]).

This last point is the one which interests us the most. More information on the biological role of the astrocytes can be found in [12].

Cornell-Bell et al. [2] first remarked an increase of Ca^{2+} concentration inside the astrocytes when a glutamate stimulus is received. Moreover, they found out that the concentration of calcium ions tends to have an oscillatory pattern in time. This observation has been corroborated by in-situ studies such as [13]. The glutamate stimulus acts on the calcium concentration through the release, at the level of the membrane, of inositol trisphosphate (IP3 for simplicity) into the cytoplasm, as found by [7]. This soluble messenger is transported towards the endoplasmatic reticulum of the astrocytes where it triggers the opening of the calcium channels, creating a flux of ions from the endoplasmatic reticulum into the cytoplasm [8]. The incrase of cytosolic calcium triggers the release of arachidonic acid from the membrane phospholipides with many consequences on the surrouding tissues (see [8] and the references therein).

There are currently many models to address the issue of calcium ions dynamics in an astrocyte: we cite, in order of publishing date [3], [9], [17] and finally [8]. These studies have been conducted using reduced order models, where only ODEs are employed. The strenght of this approach is the (relative) simplicity of the mathematics behind the model which then allows to consider many regulatory phenomena. On the other hand, the main disadvantage is that, considering the availability of data concerning the spatial concentration of Ca^{2+} ions (especially in vegetal cells), the right context to study these phenomena involves both space and time.

1.2 Our contribution

We aim at providing a first highly simplified model to study the dynamics of Ca^{2+} ions, whose release is triggered by the IP3 stimulus in a space extended context, namely 2D and/or 3D. To the best of our knowledge, this kind of model is new in litterature.

This model does not aim at being complete and taking all the relevant biological processes into account. We conceive it as a basic framework which can ease the creation of more complex models, once the most basic one are completely understood. This has been done knowing that adding the spatial dimension would result in a complexification of the overall model.

In [16], five main contributions to the calcium ions dynamics are identified. They are:

- **Calcium flux through transmembrane calcium channels**. These channels act by passive transport induced by the difference of concentration between the area outside the cell (high concentration) and the cytosol (low concentration), producing a net influx of ions.

- Calcium flux through the transmembrane calcium pumps mediated by adenosine triphosphate (ATP). This constitutes an active transport obtained by energy consumption.

- Calcium uptake by the receptors localized over the endoplasmatic reticulum membrane. Mechanism acting against the natural diffusion which drives calcium from the endoplasmatic reticulum (high concentration) to the cytosol (low concentration).

- **Calcium release from the channels localized over the endoplasmatic reticulum membrane.** This is modulated by the level of IP3 that is produced by the glutamate receptors located on the cell membrane.
- Active transport of calcium from the cytosol to the extracellular site. This process is mediated by the neuron nearby the astrocyte.

In our multidimensional model, only the processes in **bold** will be taken into account. In particular, they are modeled in terms of time varying local boundary conditions, whereas the concentrations satisfy a time-dependent diffusion equation with constant diffusivity. Tough we have kept the model as simple as possible by considering only the diffusion of the calcium ions and the IP3, it is evident that it can be enriched by considering the electric field and its effect on the charged particles, as well as other phenomena.

Finally, we discretize our model in time using Finite Differences and in space using Finite Elements, in order to obtain some numerical results. For this purpose, we resort to the `FEMOS-MP` (Finite Element Modeling-Oriented Simulator for Multi-Physics simulations) platform [10, 11]. `FEMOS-MP` is a general-purpose modular code based on the Galerkin FE method to model complex interplaying multiphysics phenomena in semiconductor and biophysics, including both 2D and 3D geometric configurations.

2 Models

2.1 Continum model

2.1.1 Domain

We consider a highly simplified geometry for an astrocyte, where it is seen as a circle (in 2D) or a sphere (in 3D) of radius R_{cyt}. For the sake of simplicity, it contains only an endoplasmatic reticulum (ER) which is circular/spherical of radius R_{er} with the same center.

The overall cellular domain is $\Omega = \Omega_{\text{cyt}} \cup \Omega_{\text{er}}$, where Ω_{cyt} is the volume of the cythosol excluding the endoplasmatic reticulum and Ω_{er} is the volume containing the endoplasmatic reticulum. These volumes are divided by the boundary Γ_{in} given by:

$$\Gamma_{\text{in}} = \overline{\Omega_{\text{cyt}}} \cap \overline{\Omega_{\text{er}}}, \tag{1}$$

and we consider its proper subset $\Gamma_{\text{in,c}} \subset \Gamma_{\text{in}}$ which reprensents the channels through which the calcium can be released from the ER towards the cytoplasm.

The external boundary of the astrocyte Γ_{ext} given by:

$$\Gamma_{\text{ext}} = \partial \left(\Omega_{\text{cyt}} \cup \overline{\Omega_{\text{er}}} \right), \tag{2}$$

and is divided into three parts, $\Gamma_{\text{ext,c}}$ the calcium channels, $\Gamma_{\text{ext,r}}$ the glutamate receptors from which we observe an inlet of IP3 molecules, and the remaining part of the boundary. One can consider Figure 1 for a visual intuition of our geometry.

2.1.2 The IP3 problem

As we hinted before, we consider that the IP3 molecules are only subjected to a time-depending diffusion process with constant diffusivity. Thus, the problem for the con-

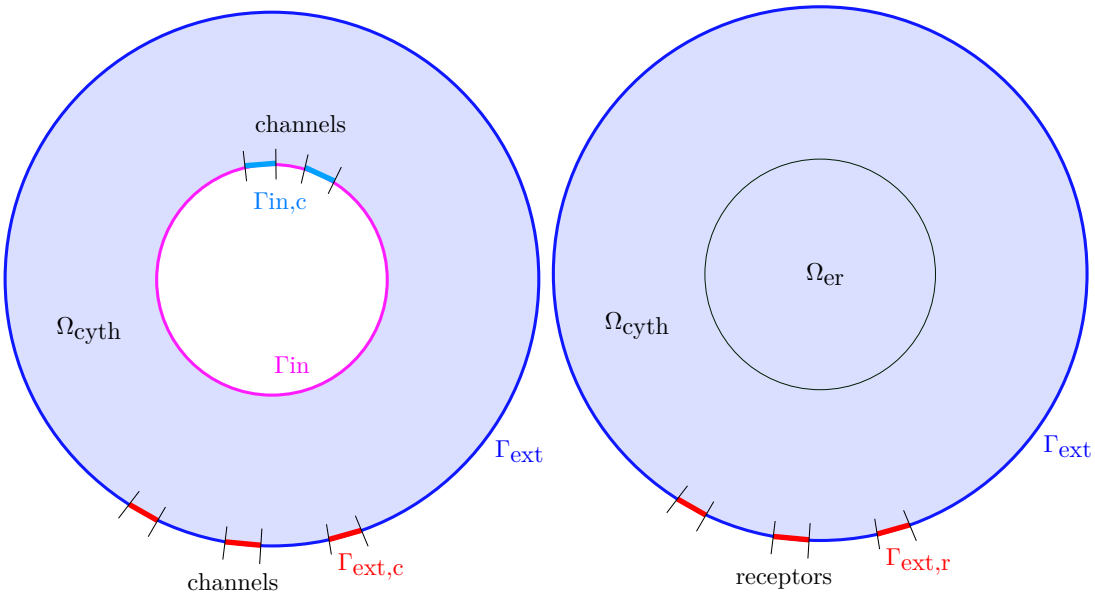

Figure 1: On the left: holed domain used for the calcium computation, where Γ_{ext} is the external boundary of the system and the boundary Γ_{in} represents the interface between the interior of the cell and the endoplasmatic reticulum. On the right: full domain used for the computations concerning the IP3. We observe that the calcium channels and the IP3 receptors on the external boundary do not coincide.

centration ψ_{IP3} of IP3 reads:

$$\begin{cases} \frac{\partial \psi_{\text{IP3}}}{\partial t}(t,\mathbf{x}) - D_{\text{IP3}}\Delta\psi_{\text{IP3}}(t,\mathbf{x}) = 0 & \text{for} \quad (t,\mathbf{x}) \in [0,T] \times \Omega_{\text{cyt}} \cup \Omega_{\text{er}} \\ \psi_{\text{IP3}}(t,\mathbf{x}) = \langle \psi_{\text{IP3}} \rangle & \text{for} \quad (t,\mathbf{x}) \in [0,T] \times \Gamma_{\text{ext}} - \Gamma_{\text{ext,r}} \\ -D_{\text{IP3}}\nabla\psi_{\text{IP3}}(t,\mathbf{x}) \cdot \mathbf{n} = \sigma(t) & \text{for} \quad (t,\mathbf{x}) \in [0,T] \times \Gamma_{\text{ext,r}}, \end{cases} \tag{3}$$

where $D_{\text{IP3}} > 0$ is the diffusion coefficient of the species, $T > 0$ is the final time, $\langle \psi_{\text{IP3}} \rangle$ is the baseline value of the concentration, $\mathbf{n}$ is the normal vector to the boundary of the domain and $\sigma(t)$ is the IP3 stimulus which can be triggered during the simulation. The initial datum is taken as a constant concentration:

$$\psi_{\text{IP3}}(t=0,\mathbf{x}) = \langle \psi_{\text{IP3}} \rangle . \tag{4}$$

Concerning the modeling of the stimulus, we can envision a constant stimulation of intensity $\overline{\sigma} > 0$ coming at time t_{stim} for the duration of $\Delta t_{\text{stim}} > 0$, which reads:

$$\sigma(t) = \begin{cases} \overline{\sigma} & \text{for} \quad t_{\text{stim}} \leq t < t_{\text{stim}} + \Delta t_{\text{stim}} \\ 0 & \text{elsewhere.} \end{cases} \tag{5}$$

Inded, we do not model the process through which a glutamate stimulus forces the release of IP3 but we just consider that, at some time, IP3 molecules are diffused starting from the cellular membrane. From our point of view, the best simple boundary condition to model a flux of moleculs though the boundary is the Neumann boundary condition.

2.1.3 The calcium problem

Following the same idea of the IP3, the equations for the concentration of Ca^{2+} ions ($\psi_{Ca^{2+}}$) are:

$$\begin{cases} \frac{\partial \psi_{Ca^{2+}}}{\partial t}(t,\mathbf{x}) - D_{Ca^{2+}}\Delta\psi_{Ca^{2+}}(t,\mathbf{x}) = 0 & \text{for} \quad (t,\mathbf{x}) \in [0,T]\times\Omega_{cyt} \\ \psi_{Ca^{2+}}(t,\mathbf{x}) = \left\langle \psi_{Ca^{2+}} \right\rangle_{cyt} & \text{for} \quad (t,\mathbf{x}) \in [0,T]\times\Gamma_{ext} - \Gamma_{ext,c} \\ \psi_{Ca^{2+}}(t,\mathbf{x}) = \left\langle \psi_{Ca^{2+}} \right\rangle_{cyt} & \text{for} \quad (t,\mathbf{x}) \in [0,T]\times\Gamma_{in} - \Gamma_{in,c} \\ -D_{Ca^{2+}}\nabla\psi_{Ca^{2+}}(t,\mathbf{x})\cdot\mathbf{n} = g_{in}^{nat} + g_{in}^{stim}(\psi_{IP3}(t,\mathbf{x})) & \text{for} \quad (t,\mathbf{x}) \in [0,T]\times\Gamma_{in,c} \\ -D_{Ca^{2+}}\nabla\psi_{Ca^{2+}}(t,\mathbf{x})\cdot\mathbf{n} = g_{ext}^{nat} & \text{for} \quad (t,\mathbf{x}) \in [0,T]\times\Gamma_{ext,c}, \end{cases} \tag{6}$$

where $\left\langle \psi_{Ca^{2+}} \right\rangle_{cyt}$ is the baseline concentration inside the cytosol and $\left\langle \psi_{Ca^{2+}} \right\rangle_{er}$ is that for the endoplasmatic reticulum. On the other hand g_{ext}^{nat} and g_{in}^{nat} are the unstimulated fluxes of ions and $g_{in}^{stim}(\psi_{IP3}(t,\mathbf{x}))$ accounts for the release due to the stimulation by the increased concentration of IP3. It is worthwhile to observe that now the problem is solved only in the cytosol, namely in Ω_{cyt}. The initial condition reads:

$$\psi_{Ca^{2+}}(t=0,\mathbf{x}) = \left\langle \psi_{Ca^{2+}} \right\rangle_{cyt}. \tag{7}$$

Observe that the second boundary condition could be taken as a Neumann boundary condition in order to model the spontaneous diffusion of calcium from the endoplasmatic reticulum to the cytoplasm induced by the difference of concentration, adding a contribution which is not only localized on $\Gamma_{in,\,c}$ with a flux g_{in}^{nat}. We decided not to do it to keep the model as simple as possible.

In order to model the triggered release g_{in}^{stim}, we can consider that if the mean value of the concentration of IP3 of the boundary $\Gamma_{in,r}$ goes beyond a certain threshold value $\psi_{IP3}^{thr} > 0$, the calcium is released into the cytoplasm from the endoplasmatic reticulum with a rate $\overline{g_{in}^{stim}} > 0$:

$$g_{in}^{stim}(\psi) = \begin{cases} \overline{g_{in}^{stim}} & \text{if} \quad \left(\fint_{\Gamma_{in,r}} \psi \, d\gamma\right) > \psi_{IP3}^{thr} \\ 0 & \text{otherwise.} \end{cases} \tag{8}$$

Perhaps, a simpler alternative, which is the one we use due to its easier implementation, is:

$$g_{in}^{stim}(\psi) = \begin{cases} \overline{g_{in}^{stim}} & \text{if} \quad \max_{\mathbf{x}\in\Gamma_{in,r}} \psi(\mathbf{x}) > \psi_{IP3}^{thr} \\ 0 & \text{otherwise.} \end{cases} \tag{9}$$

It is evident that we can envision a stimulated release of ions g_{in}^{stim} which is spatially dependent and can provide a more realistic model. In order to do so, it is necessary to deeply modify the computational environment `FEMOS-MP`.

2.2 Discretized model

2.2.1 Time discretization

The time discretization of the interval $[0,T]$ is done in the simplest way, considering a fixed time step $\Delta t > 0$ (possibly small compared to the diffusion time of the species, as we will formalize soon) and the sequence of discrete times t_n where:

$$t_n = n\Delta t, \tag{10}$$

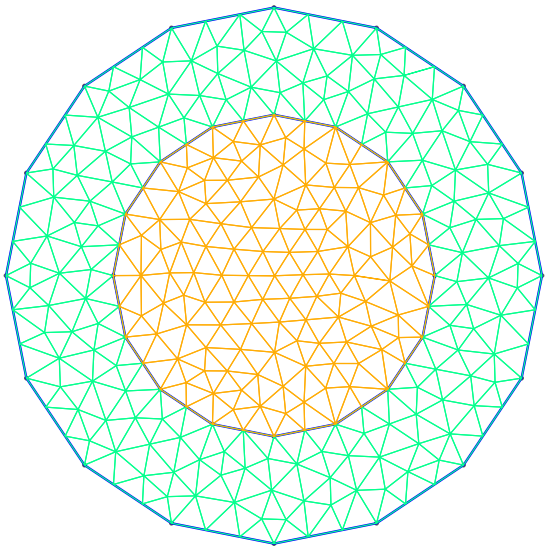

Figure 2: Example of tethraedral mesh, suitable for a finite elements discretization, generated by GMESH. In green, edges belonging to Ω_{cyt} and in orange those belonging to Ω_{er}.

for $n = 0, \dots, \lceil \frac{T}{\Delta t} \rceil$. The time derivatives in Eq. (3) and (6) are discretized at these discrete times using first-order finite differences, namely saying that:

$$\partial_t f|_{t=t_n} \simeq \frac{f^{n+1} - f^n}{\Delta t}, \tag{11}$$

where f^n is the value of a function f at time t_n, which is still a function of the space variable.

Of course, one could envision more sophisticated but also more expensive ways of treating the time variable, such as Runge-Kutta methods, which nevertheless are behond the scope of this work. See, for example, [1], for more information.

2.3 Space discretization

For the space discretization, we consider a triangular (for the 2D) or tetrahedral (for the 3D) mesh generated by the software GMESH, suitable for standard Finite Elements approximations of elliptic problems (see Figure 2 for an example). Observe that the boundary of the domains has been rectified to simplify the setting.

We do not treat the principles of the discretization by standard $\mathbb{P}_1$ Finite Elements in this context: the interested reader can find a complete introduction in [15] or equivalent books on numerical analysis. We do not need to have a deep knowledge on the subject since the spatial discretization of an elliptic problem, once the mesh is provided, is automatically handled by FEMOS-MP. This is the reason why we provide only semi-discretized models where the spatial approximation procedure is understood.

2.3.1 The IP3 discretized model

Using first-order finite differences in time as previously indicated, we obtain the following problem at time step t_n:

$$\begin{cases} \frac{1}{\Delta t}\psi_{\text{IP3}}^{n+1}(\mathbf{x}) - D_{\text{IP3}}\Delta\psi_{\text{IP3}}^{n+1}(\mathbf{x}) = \frac{1}{\Delta t}\psi_{\text{IP3}}^{n}(\mathbf{x}) & \text{in} \quad \Omega_{\text{cyt}} \cup \Omega_{\text{er}} \\ \psi_{\text{IP3}}^{n+1}(\mathbf{x}) = \langle \psi_{\text{IP3}} \rangle & \text{on} \quad \Gamma_{\text{ext}} - \Gamma_{\text{ext,r}} \\ -D_{\text{IP3}}\nabla\psi_{\text{IP3}}^{n+1}(\mathbf{x}) \cdot \mathbf{n} = \sigma(t^n) & \text{on} \quad \Gamma_{\text{ext,r}}, \end{cases} \tag{12}$$

where the unknown to be computed is ψ_{IP3}^{n+1}. It is interesting to observe that this problem is independent from the calcium problem and thus can be solved independently.

For this case, we show how to recover the variational formulation of Eq. (12), from which the Finite Element approximation originates. For the sake of simplicity, take $\langle \psi_{\text{IP3}} \rangle = 0$ (otherwise use a lifting) and consider the Sobolev space:

$$V = H^1_{\Gamma_{\text{ext}} - \Gamma_{\text{ext,r}}} := \left\{ \phi \in L^2(\Omega) \ : \ \nabla\phi \in \left[L^2(\Omega)\right]^2 \quad \text{and} \quad \phi|_{\Gamma_{\text{ext}} - \Gamma_{\text{ext,r}}} = 0 \right\}, \tag{13}$$

where the gradient is taken in the weak sense (seen as a distribution acting via duality product on a regular function) and the value of ϕ on the boundary is taken in the sense of the trace. Let us multiply the first equation of (12) and formally integrate by parts. We obtain:

$$\frac{1}{\Delta t}\int_\Omega \psi_{\text{IP3}}^{n+1}(\mathbf{x})\phi(\mathbf{x})d\mathbf{x} - \int_\Omega D_{\text{IP3}}\Delta\psi_{\text{IP3}}^{n+1}(\mathbf{x})\phi(\mathbf{x})d\mathbf{x} = \frac{1}{\Delta t}\int_\Omega \psi_{\text{IP3}}^{n}(\mathbf{x})\phi(\mathbf{x})d\mathbf{x} \tag{14}$$

$$= \frac{1}{\Delta t}\int_\Omega \psi_{\text{IP3}}^{n+1}(\mathbf{x})\phi(\mathbf{x})d\mathbf{x} + \int_\Omega D_{\text{IP3}}\nabla\psi_{\text{IP3}}^{n+1}(\mathbf{x}) \cdot \nabla\phi(\mathbf{x})d\mathbf{x} + \int_{\Gamma_{\text{ext,r}}} \sigma(t^n)\phi(\mathbf{x})d\mathbf{x}, \tag{15}$$

where we have used the fact that the test function ϕ vanishes on a part of the boundary. The weak formulation is:

$$\begin{aligned} &\text{Find } \psi_{\text{IP3}}^{n+1} \in V \quad \text{such that} \quad \forall \phi \in V \\ &\frac{1}{\Delta t}\int_\Omega \psi_{\text{IP3}}^{n+1}(\mathbf{x})\phi(\mathbf{x})d\mathbf{x} + \int_\Omega D_{\text{IP3}}\nabla\psi_{\text{IP3}}^{n+1}(\mathbf{x}) \cdot \nabla\phi(\mathbf{x})d\mathbf{x} + \int_{\Gamma_{\text{ext,r}}} \sigma(t^n)\phi(\mathbf{x})d\mathbf{x} \\ &= \frac{1}{\Delta t}\int_\Omega \psi_{\text{IP3}}^{n}(\mathbf{x})\phi(\mathbf{x})d\mathbf{x}. \end{aligned}$$

One can show by using the Lax-Milgram theorem that this problem is indeed well-posed in the sense of Hadamard if we assume, for example, that

$$\sigma \in L^\infty([0,T]), \tag{16}$$

which is highly reasonable and always verified with our choice.

Since the Galerkin approximation is an internal approximation, namely the finite dimensional approximation space V_h is such that

$$V_h \subset V, \tag{17}$$

the variational formulation is exactly what we use to seek a Finite Element approximation and becomes a linear algebraic system, since the number of test function $\phi_h \in V_h$ is now finite.

2.3.2 The calcium discretized model

Doing the same for the calcium ions, we obtain:

$$\begin{cases} \frac{1}{\Delta t}\psi^{n+1}_{Ca^{2+}}(\mathbf{x}) - D_{Ca^{2+}}\Delta\psi^{n+1}_{Ca^{2+}}(\mathbf{x}) = \frac{1}{\Delta t}\psi^{n}_{Ca^{2+}}(\mathbf{x}) & \text{in} \quad \Omega_{cyt} \\ \psi^{n+1}_{Ca^{2+}}(\mathbf{x}) = \left\langle \psi_{Ca^{2+}} \right\rangle_{cyt} & \text{on} \quad \Gamma_{ext} - \Gamma_{ext,c} \\ \psi^{n+1}_{Ca^{2+}}(\mathbf{x}) = \left\langle \psi_{Ca^{2+}} \right\rangle_{cyt} & \text{on} \quad \Gamma_{in} - \Gamma_{in,c} \\ -D_{Ca^{2+}}\nabla\psi^{n+1}_{Ca^{2+}}(\mathbf{x})\cdot\mathbf{n} = g^{nat}_{in} + g^{stim}_{in}\left(\psi^{n+1}_{IP3}(\mathbf{x})\right) & \text{on} \quad \Gamma_{in,c} \\ -D_{Ca^{2+}}\nabla\psi^{n+1}_{Ca^{2+}}(\mathbf{x})\cdot\mathbf{n} = g^{nat}_{ext} & \text{on} \quad \Gamma_{ext,c}, \end{cases} \tag{18}$$

where we decided to discretize the influx of calcium from the endplasmatic reticulum in this way since the value of $\psi_{IP3}(t,\mathbf{x})$ is available at the new time step by solving Eq. 12.

Observe that in both diffusion problems, the Laplacian operator has been discretized implicitely in time, in order to have an unconditionally stable scheme, so that we can chose whatever Δt.

The recovery of the variational formulation for this problem follows the same idea than for the IP3, so we do not repeat it. We just observe that a useful assumption to ease the proof of well-posedness of the problem is:

$$g^{stim}_{in} \in L^{\infty}(\mathbb{R}_{+}). \tag{19}$$

3 Parameters of the model

In this section, we try to recover the parameters employed in the previous numerical model. We observe that these values are recovered in a very simple way from what is available in litterature. Thus, there is a considerable latitude for improving this in the framework of a joint study with biologists and physiologist in order to adapt them to the specific context one wants to simulate. The values we provide should be seen as "orders of magnitude".

3.1 Domain and simulation time

3.1.1 Geometry

As we have suggested before, the whole astrocyte is supposed to be spherical of volume (taken from [5]):

$$V = 5.2\cdot 10^{-10}\ \text{cm}^3. \tag{20}$$

Since we consider the cell to be split into two compartments, namely the cytosol (of volume V_{cyt}) and the endoplasmatic reticulum (of volume V_{er}), we have that:

$$V = V_{cyt} + V_{er} \qquad \frac{V_{cyt}}{V_{er}} = 3.5, \tag{21}$$

where the volume ratio has been taken from [14]. We consider a spherical symmetry both for the cytosol and the endoplasmatic reticulum, whose radii are respectively R_{cyt} and R_{er}. Simple algebra yields:

$$R_{er} = \left(\frac{V}{6\pi}\right)^{1/3} \simeq 3.0\cdot 10^{-4}\ \text{cm}, \tag{22}$$

and

$$R_{\text{cyt}} = \left(\frac{7V}{12\pi}\right)^{1/3} \simeq 4.6 \cdot 10^{-4} \text{ cm}. \tag{23}$$

Considering the channels on the different boundaries, we do not perform a study concerning their shape and size. Though we have used few channels with a size comparable to the radii we have found (thus "macroscopic" channels compared to the size of cell) for the sake of simplicity, we consider that a more realistic situation would be to consider a large amount of small "microscopic" channels. The input file given to `GMESH` is shown in Figure 5 and 6 for the sake of completeness. This is certainly a subject of great improvement of the model.

3.1.2 Simulation time

The overall simulation time T and the time step Δt are taken as:

$$T = 0.015 \text{ s} \qquad \Delta t = T/300, \tag{24}$$

in order to ensure that we have:

$$T \gtrsim \max\left(\tau_{\text{IP3}}, \tau_{\text{Ca}^{2+}}\right) \qquad \text{and} \qquad \Delta t \ll \min\left(\tau_{\text{IP3}}, \tau_{\text{Ca}^{2+}}\right), \tag{25}$$

in order to capture the whole diffusion process for both species.

3.2 IP3

3.2.1 Baseline concentration

We first express the baseline concentrations in terms of number of particles over cube centimeter. On the other hand, in the lumped models (0D), which are the most common framework for this kind of problem (see references cited at the beginning), these values are provided in molar concentrations, namely moles over litre, thus a conversion though the Avogadro's number $N_A = 6.022 \cdot 10^{23} \text{ mol}^{-1}$ is necessary.

Concerning the baseline concentration of IP3 inside the cell, which will be used as initial datum for the numerical simulation, we take:

$$\langle \psi_{\text{IP3}} \rangle = 5.0 \cdot 10^{-7} \text{mol/l} \cdot 6.022 \cdot 10^{23} 1/\text{mol} \simeq 3.0 \cdot 10^{14} \frac{1}{\text{cm}^3}, \tag{26}$$

starting from the value given by [16].

3.2.2 Diffusion coefficient and diffusion time

The diffusion coefficient is taken from [4]:

$$D_{\text{IP3}} = 280 \, \frac{\mu\text{m}^2}{\text{s}} = 2.8 \cdot 10^{-6} \, \frac{\text{cm}^2}{\text{s}}. \tag{27}$$

Once the diffusion constant is known, it is important to estimate the diffusion time of the species. Which provides an idea of the time scale on which the concentration profile homogenizes. Simple dimensional arguments estimate the diffusion time, in a problem of typical length-scale L and with diffusivity D as:

$$\tau = \frac{L^2}{2D}. \tag{28}$$

Thus, for the IP3, we recover:

$$\tau_{\text{IP3}} = \frac{\left(R_{\text{cyt}} - R_{\text{er}}\right)^2}{2D_{\text{IP3}}} \simeq 4.6 \cdot 10^{-3} \text{ s}, \tag{29}$$

since even if we simulate what happens inside the endoplasmatic reticulum just not to enforce not "natural" conditions for the IP3 on Γ_{int}, we are not interested in what happens inside this compartment.

Hence, we will select a time-step way smaller than $\min\left(\tau_{\text{IP3}}, \tau_{\text{Ca}^{2+}}\right)$ in order to observe the diffusion doing its work.

3.2.3 Boundary conditions

We have to select the stimulated flux $\overline{\sigma}$ of IP3. The guide principle is that the concentration of IP3 must reach – during stimulation – the concentration of 1.5 μM observed by [16]. This is equivalent, with our units, to obtain a concentration of (at least) $9.0 \cdot 10^{14} \frac{1}{\text{cm}^3}$, which is three times the baseline concentration by Eq. (26).

This has to be obtained taking the stimulation time Δt_{stim} in consideration. Let us take

$$t_{\text{stim}} = 30\Delta t \qquad \Delta t_{\text{stim}} = 30\Delta t. \tag{30}$$

Performing numerical simulations only for the IP3, we have observed that a good choice is:

$$\overline{\sigma} = 1.148 \cdot 10^{-1}. \tag{31}$$

This grants to observe a IP3 front travelling towards the endoplasmatic reticulum which is sufficient to excitate the release of calcium ions at some time, but is not sufficient to keep the threshold level (given by Eq. (42)) for the whole simulation. Thus, we also observe a comeback to the "rest" state.

Observe that this value needs to be changed whenever the parameters of the stimulation given by Eq. (30) or other parameters of the system are changed. This is due to the fact that for the time-varying heat equation, the influence of the boundary fluxes on the solution is strictly linked with the notion of time.

3.3 Calcium

3.3.1 Baseline concentrations

We first express the baseline concentrations taken from [16] in terms of number of particles over cube centimeter. This gives:

$$\left\langle \psi_{\text{Ca}^{2+}} \right\rangle_{\text{cyt}} = 1.0 \cdot 10^{-7} \text{ mol/l} \cdot 6.022 \cdot 10^{23} \text{ 1/mol} \simeq 6.0 \cdot 10^{13} \frac{1}{\text{cm}^3} \tag{32}$$

$$\left\langle \psi_{\text{Ca}^{2+}} \right\rangle_{\text{er}} = 2.0 \cdot 10^{-6} \text{ mol/l} \cdot 6.022 \cdot 10^{23} \text{ 1/mol} \simeq 1.2 \cdot 10^{15} \frac{1}{\text{cm}^3} \tag{33}$$

$$\left\langle \psi_{\text{Ca}^{2+}} \right\rangle_{\text{ext}} = 2.5 \cdot 10^{-3} \text{ mol/l} \cdot 6.022 \cdot 10^{23} \text{ 1/mol} \simeq 1.5 \cdot 10^{18} \frac{1}{\text{cm}^3} \tag{34}$$

We observe that there is a quite substantial difference between the concentration inside the cell and that in the sourrounding area. These baseline concentrations are used as initial condition as far as the cytoplasm is concerned and to compute the natural calcium fluxes though the boundary of the domain.

3.3.2 Diffusion coefficient and diffusion time

The diffusion coefficient for the calcium ions is taken from [6]:

$$D_{Ca^{2+}} = 5.3 \cdot 10^{-6} \text{ cm}^2 \text{ s}^{-1}. \tag{35}$$

From this, we can recover the characteristic diffusion time of the species $\tau_{Ca^{2+}}$ given by:

$$\tau_{Ca^{2+}} = \frac{\left(R_{cyt} - R_{er}\right)^2}{2D_{Ca^{2+}}} \simeq 2.4 \cdot 10^{-3} \text{ s}, \tag{36}$$

which provides a useful estimation of the time needed for the simulation, at least when only diffusion phenomena are involved.

3.3.3 Boundary conditions

In order to estimate g_{ext}^{nat}, namely the natural flux of calcium from the exterior of the cell to the cytoplasm passing though the channels, we consider that at each boundary, the concentration variation takes places in the direction given by $\mathbf{n}$, thus we reduce the computation to a one-dimensional problem. The idea is to approximate the normal derivative with a Finite Difference over the thickness of the membrane, as if the concentration profile though the channel were an affine function of the position in the channel. We enforce:

$$g_{ext}^{nat} = -D_{Ca^{2+}} \frac{\left\langle \psi_{Ca^{2+}} \right\rangle_{ext} - \left\langle \psi_{Ca^{2+}} \right\rangle_{cyt}}{t_m} \simeq -D_{Ca^{2+}} \frac{\left\langle \psi_{Ca^{2+}} \right\rangle_{ext}}{t_m} \tag{37}$$

$$\simeq -2.0 \cdot 10^{19} \frac{1}{\text{s cm}^2}, \tag{38}$$

where t_m is the thickness of a cellular membrane (here 4.0 nm as order of magnitude). The minus sign is given, as we expect, by the fact that the concentration gradient pushes the calcium inside the cell, going in the opposite direction with respect to the normal vector $\mathbf{n}$.

Using the same procedure for the other boundary Γ_{in}, we obtain:

$$g_{in}^{nat} = -D_{Ca^{2+}} \frac{\left\langle \psi_{Ca^{2+}} \right\rangle_{er} - \left\langle \psi_{Ca^{2+}} \right\rangle_{cyt}}{t_m} \simeq \tag{39}$$

$$\simeq -1.5 \cdot 10^{16} \frac{1}{\text{s cm}^2}, \tag{40}$$

In this last case, we assume that the transition between the cytoplasm and the endoplasmatic reticulum takes place on a characteristic length with the same value than t_m.

For the triggered flux, the simpler choice we can make is to consider that, according to the observations made by [16], we want to increase the calcium concentration close to the endoplasmatic reticulum of one order of magnitude. Thus, for the sake of simplicity, we consider:

$$\overline{g_{in}^{stim}} = 10\, g_{int}^{nat} \simeq 1.5 \cdot 10^{17} \frac{1}{\text{s cm}^2}. \tag{41}$$

Finally, we are left to determine the trigger constant ψ_{IP3}^{thr} which starts the release of ions from the endoplasmatic reticulum. will be taken in order to carry the simulation in accordance with what we have seen in the lumped model by [16], namely:

$$\psi_{IP3}^{thr} = 1.5 \cdot 10^{-6} \text{mol/l} \cdot 6.022 \cdot 10^{23} 1/\text{mol} \simeq 9.0 \cdot 10^{14} \frac{1}{\text{cm}^3}, \tag{42}$$

which was the value we had found in the Section dedicated to the IP3 as the value we want to reach by stimulation.

Caveat The values for the fluxes we have found before have been obtained by a static approach. Once we start simulating, we understand, as we already emphasized for the IP3, that the time plays a huge role when Neumann bondary conditions are involved. Thus, the value we found are indeed huge compared to the orders of magnitude we expenct and moreover, they lead to the instability of the solver.

The value of these parameters has to be adjusted considering the observation time T one desires and should be based on in-vivo biological measures. Progressively tuning the fluxes thanks to simulations, we retain:

$$g_{\text{ext}}^{\text{nat}} = 1.59 \cdot 10^{-2} \qquad g_{\text{in}}^{\text{nat}} = 1.06 \cdot 10^{-2} \qquad \overline{g_{\text{in}}^{\text{stim}}} = 1.06 \cdot 10^{-1}. \tag{43}$$

4 Results

A possible numerical outcome is shown on Figure 3 and 4. Here, we have put in evidence the isoline (in white) corresponding to the threshold value of IP3. In the first frame, the IP3 stimulation starts from the boundary and diffuses towards the endoplasmatic reticulum. In the second frame, it is about to reaching it and starting the release of calcium ions into the cytosol. This is what we observe in the third and fourth frame. In the latter, we remark that even if the stimulation is no longer present, the magnitude of the past one is enough to continue the release phenomenon for some time. In the last frame, we see that the concentration falls under the threshold, thus the original framework is re-established.

5 Comments, perspectives and conclusion

5.1 Comments

In this work, we have observed how a simple model can represent a **stimulation phenomenon** triggered by the concentration of a certain species. As we already mentioned, this is a "far-from-reality" modelization which pretends to be nothing but a starting point for more complex models.

These weeks of work have shown how strongly, even if the model is kept as simple as possible and everything seems clear, we need observations and **data**. Without them, the model cannot show its predictive power and we are almost unable to test it against empirical observations.

5.2 Perspectives

These are the perspectives that we envision to boost the quality of this research:

- **Deeper modification of the solver**. This is probably the most basic development we can envision. Our work has been conducted using `FEMOS-MP`, modifying pieces of code "by hand". This way of proceeding is not suitable when considering many different parameters (think about different stimulation times) and one should make this automatic by letting the user providing them in the input file.

- **Find better parameters**. As told before, this is probably the most crucial point in this subject. We can figure out two main aspects, namely:
  - Cooperation with biologist to obtain data and images from in-vivo. The interest of these data is invaluable, since they provide a spatial and temporal description, which is exactly the framework of our model.
  - Parametric identification through inverse problem. We try to match the observations mentioned before by repeated Finite Elements simulations, driving the parameters of the model towards the minimization of a cost functional representing a "distance" between the outcome of the simulation and the observations. It could be something like:

$$J\left(u_{\text{sim}}[\mathbf{p}]\right) = \int_{\Omega} \left|u_{\text{obs}}(\mathbf{x}) - u_{\text{sim}}[\mathbf{p}](\mathbf{x})\right|^2 d\mathbf{x}, \tag{44}$$

    where the simulated solution depends on a vector of parameters $\mathbf{p} \in \mathcal{K} \subset \mathbb{R}^q$, where $\mathcal{K}$ is a compact. The problem we could analyze is:

$$\text{Find} \quad \mathbf{p}^* = \text{argmin}_{\mathbf{p}\in\mathcal{K}} J\left(u_{\text{sim}}[\mathbf{p}]\right). \tag{45}$$

    These kind of issue is quite common in mechanics, where we postulate a constitutive law for a material and we try to recover its parameters by matching simulations and data from specimens.

- **A more accurate geometric description** of the cell, in terms of shape of the domain and the channels. Again, this can be achieved, probably more easily than the previous point, thanks to a joint work with biologists. As already said, we think that channels should be more but way smaller than what we have considered.

- **Construct an enriched model**. An ambitious aim could be to recover an oscillatory behavior even for non-periodic stimulations (like the one we used), as observed for the ODE models. It is evident that with simple diffusion, we cannot achieve this. Possible explorations include:
  - Enlarge the set of phenomena encoded by the equations. For example, one can also consider the electric field, since the calcium ions are charged and the channels can contain fixed charges. Another interesting model could be the introduction of some non-linear reaction term in the equation, which could be responsible for the formation of spiral waves (which are periodic phenomena), solitons and other non-linear structures. These structures could interact with the specific "donought-like" shape of the cell to generate a pulsatile behavior.
  - Consider more articulate boundary conditions, namely localized one, which are varying in time according to the local concentrations. This avoids, in case of spatial inhomogeneities (that we have avoided) to have a non-local effect of the stimulation, which is indeed non-physical.

5.3 Conclusion

We have observed that the problem is quite hard to tune since the number of variables playing a role is very high, due to the fact that both space and time are involved. With

this idea in mind, we have suggested several ways of improving the model in order to be really capable of using it as a prediction tool.

Finally, I would like to deeply thank Professor Aurelio Giancarlo Mauri for having proposed this subject, having provided the already-written code of `FEMOS-MP`, for his kind help whenever I had a question and for having understood and accepted the difficulties of distance working.

References

[1] BUTCHER, J. C. *The numerical analysis of ordinary differential equations: Runge-Kutta and general linear methods*. Wiley-Interscience, 1987.

[2] CORNELL-BELL, A. H., FINKBEINER, S. M., COOPER, M. S., AND SMITH, S. J. Glutamate induces calcium waves in cultured astrocytes: long-range glial signaling. *Science 247*, 4941 (1990), 470–473.

[3] DE YOUNG, G. W., AND KEIZER, J. A single-pool inositol 1, 4, 5-trisphosphate-receptor-based model for agonist-stimulated oscillations in ca2+ concentration. *Proceedings of the National Academy of Sciences 89*, 20 (1992), 9895–9899.

[4] DICKINSON, G. D., ELLEFSEN, K. L., DAWSON, S. P., PEARSON, J. E., AND PARKER, I. Hindered cytoplasmic diffusion of inositol trisphosphate restricts its cellular range of action. *Sci. Signal. 9*, 453 (2016), ra108–ra108.

[5] DING, X., ZHANG, X., AND JI, L. Contribution of calcium fluxes to astrocyte spontaneous calcium oscillations in deterministic and stochastic models. *Applied Mathematical Modelling 55* (2018), 371 – 382.

[6] DONAHUE, B. S., AND ABERCROMBIE, R. Free diffusion coefficient of ionic calcium in cytoplasm. *Cell calcium 8*, 6 (1987), 437–448.

[7] FILOSA, J. A., AND BLANCO, V. M. Neurovascular coupling in the mammalian brain. *Experimental physiology 92*, 4 (2007), 641–646.

[8] HADFIELD, J., PLANK, M. J., AND DAVID, T. Modeling secondary messenger pathways in neurovascular coupling. *Bulletin of mathematical biology 75*, 3 (2013), 428–443.

[9] LI, Y.-X., AND RINZEL, J. Equations for insp3 receptor-mediated [ca2+] i oscillations derived from a detailed kinetic model: a hodgkin-huxley like formalism. *Journal of theoretical Biology 166*, 4 (1994), 461–473.

[10] MAURI, A., BORTOLOSSI, A., NOVIELLI, G., AND SACCO, R. 3d finite element modeling and simulation of industrial semiconductor devices including impact ionization. *Journal of Mathematics in Industry 5*, 1 (2015), 1.

[11] MAURI, A., SACCO, R., AND VERRI, M. Electro-thermo-chemical computational models for 3d heterogeneous semiconductor device simulation. *Applied Mathematical Modelling 39*, 14 (2015), 4057–4074.

[12] NETWORKGLIA. Astrocytes (`http://www.networkglia.eu/en/astrocytes`).

[13] PASTI, L., VOLTERRA, A., POZZAN, T., AND CARMIGNOTO, G. Intracellular calcium oscillations in astrocytes: a highly plastic, bidirectional form of communication between neurons and astrocytes in situ. *Journal of Neuroscience 17*, 20 (1997), 7817–7830.

[14] PLANK, M., WALL, D., AND DAVID, T. The role of endothelial calcium and nitric oxide in the localisation of atherosclerosis. *Mathematical biosciences 207*, 1 (2007), 26–39.

[15] QUARTERONI, A., AND QUARTERONI, S. *Numerical models for differential problems*, vol. 2. Springer, 2009.

[16] SACCO, R., GUIDOBONI, G., AND MAURI, A. G. Chapter 19 - differential models in cellular functions. In *A Comprehensive Physically Based Approach to Modeling in Bioengineering and Life Sciences*, R. Sacco, G. Guidoboni, and A. G. Mauri, Eds. Academic Press, 2019, pp. 467 – 491.

[17] ULLAH, G., JUNG, P., AND CORNELL-BELL, A. H. Anti-phase calcium oscillations in astrocytes via inositol (1, 4, 5)-trisphosphate regeneration. *Cell calcium 39*, 3 (2006), 197–208.

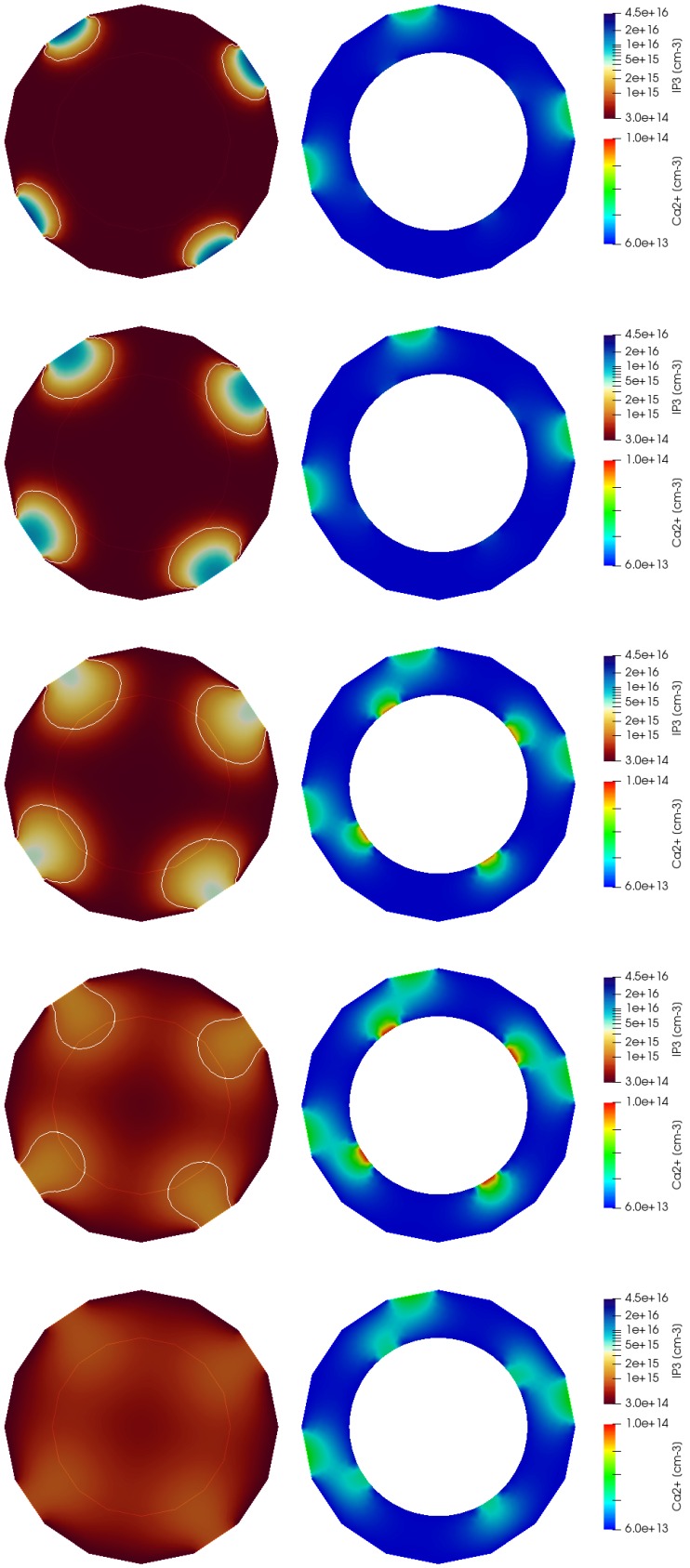

Figure 3: . Left, concentration of IP3. Right, concentration of calcium ions. From top to bottom, time steps $n = 55, 74, 100, 157, 195$. A more detailed description can be found in the text referencing this figure.

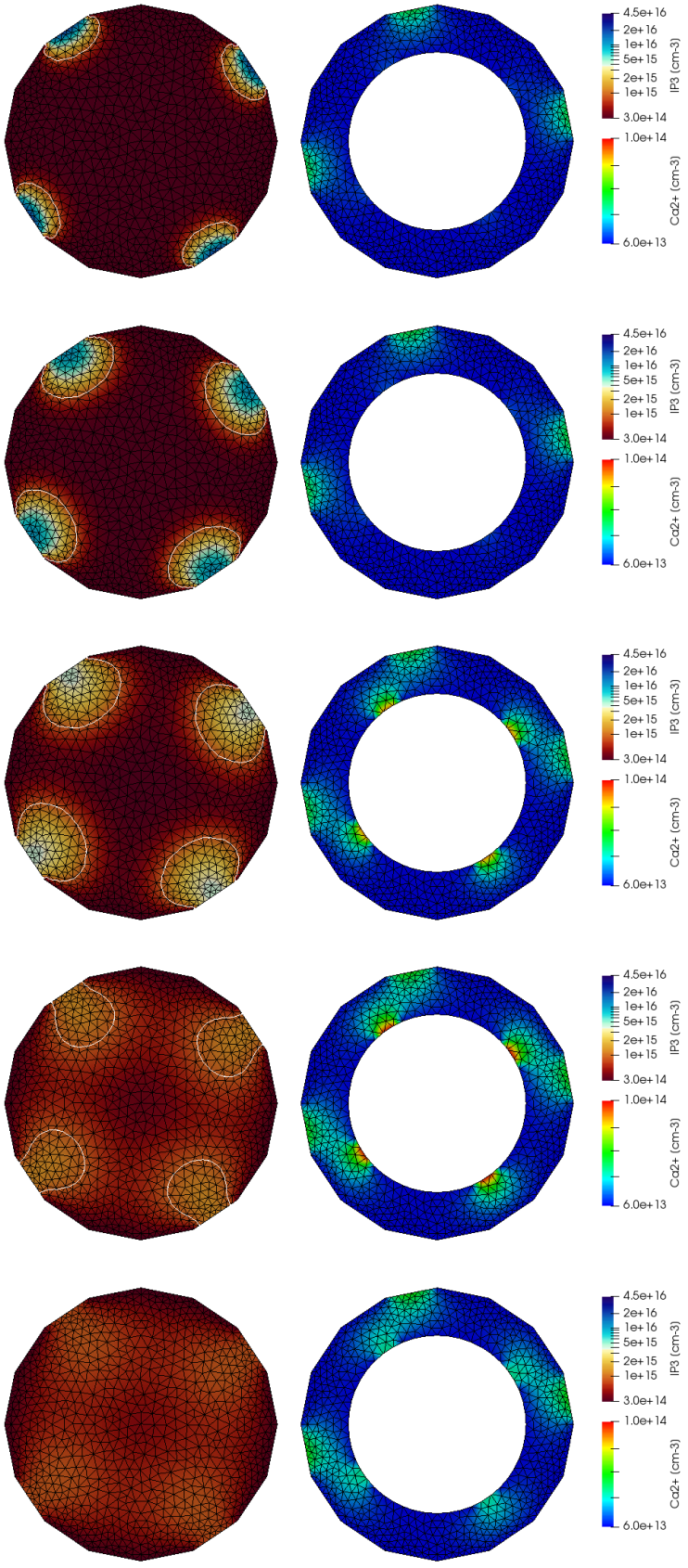

Figure 4: . Left, concentration of IP3. Right, concentration of calcium ions. From top to bottom, time steps $n = 55, 74, 100, 157, 195$.The mesh is emphasized in black.

Figure 5: Geometry file (to be continued)

```
 // Gmsh project created on Mon Jul  8 14:00:12 2019
//+
lc = 0.0005;
lc2 = 0.001;
Point(1) = {0.00046, 0, 0, lc};
//+
Point(2) = {0.00042498, 0.000176035, 0, lc};
//+
Point(3) = {0.000325269, 0.000325269, 0, lc};
//+
Point(4) = {0.000176035, 0.00042498, 0, lc};
//+
Point(5) = {0, 0.00046, 0, lc};
//+
Point(6) = {-0.000176035, 0.00042498, 0, lc};
//+
Point(7) = {-0.000325269, 0.000325269, 0, lc};
//+
Point(8) = {-0.00042498, 0.000176035, 0, lc};
//+
Point(9) = {-0.00046, 0, 0, lc};
//+
Point(10) = {-0.00042498, -0.000176035, 0, lc};
//+
Point(11) = {-0.000325269, -0.000325269, 0, lc};
//+
Point(12) = {-0.000176035, -0.00042498, 0, lc};
//+
Point(13) = {0, -0.00046, 0, lc};
//+
Point(14) = {0.000176035, -0.00042498, 0, lc};
//+
Point(15) = {0.000325269, -0.000325269, 0, lc};
//+
Point(16) = {0.00042498, -0.000176035, 0, lc};


//+
Point(17) = {0.0003, 0, 0, lc2};
//+
Point(18) = {0.000277164, 0.000114805, 0, lc2};
//+
Point(19) = {0.000212132, 0.000212132, 0, lc2};
//+
Point(20) = {0.000114805, 0.000277164, 0, lc2};
//+
Point(21) = {0, 0.0003, 0, lc2};
//+
Point(22) = {-0.000114805, 0.000277164, 0, lc2};
//+
Point(23) = {-0.000212132, 0.000212132, 0, lc2};
//+
Point(24) = {-0.000277164, 0.000114805, 0, lc2};
//+
Point(25) = {-0.0003, 0, 0, lc2};
//+
Point(26) = {-0.000277164, -0.000114805, 0, lc2};
//+
Point(27) = {-0.000212132, -0.000212132, 0, lc2};
//+
Point(28) = {-0.000114805, -0.000277164, 0, lc2};
//+
Point(29) = {0, -0.0003, 0, lc2};
//+
Point(30) = {0.000114805, -0.000277164, 0, lc2};
//+
Point(31) = {0.000212132, -0.000212132, 0, lc2};
//+
Point(32) = {0.000277164, -0.000114805, 0, lc2};
```

Figure 6: Continuation of the geometry file we used.

```
//+
Line(1) = {1, 2};
//+
Line(2) = {2, 3};
//+
Line(3) = {3, 4};
//+
Line(4) = {4, 5};
//+
Line(5) = {5, 6};
//+
Line(6) = {6, 7};
//+
Line(7) = {7, 8};
//+
Line(8) = {8, 9};
//+
Line(9) = {9, 10};
//+
Line(10) = {10, 11};
//+
Line(11) = {11, 12};
//+
Line(12) = {12, 13};
//+
Line(13) = {13, 14};
//+
Line(14) = {14, 15};
//+
Line(15) = {15, 16};
//+
Line(16) = {16, 1};


//+
Line(17) = {17, 18};
//+
Line(18) = {18, 19};
//+
Line(19) = {19, 20};
//+
Line(20) = {20, 21};
//+
Line(21) = {21, 22};
//+
Line(22) = {22, 23};
//+
Line(23) = {23, 24};
//+
Line(24) = {24, 25};
//+
Line(25) = {25, 26};
//+
Line(26) = {26, 27};
//+
Line(27) = {27, 28};
//+
Line(28) = {28, 29};
//+
Line(29) = {29, 30};
//+
Line(30) = {30, 31};
//+
Line(31) = {31, 32};
//+
Line(32) = {32, 17};


//+
Line Loop(1) = {1,2,3,4,5,6,7,8,9,10,11,12,13,14,15,16};

//+
Line Loop(2) = {17,18,19,20,21,22,23,24,25,26,27,28,29,30,31,32};

//+
Plane Surface(1) = {1, 2};
```